A Powerful Chiral Counterion Strategy for Asymmetric Transition Metal Catalysis

Gregory L. Hamilton, *et al.*

Science **317**, 496 (2007);
DOI: 10.1126/science.1145229

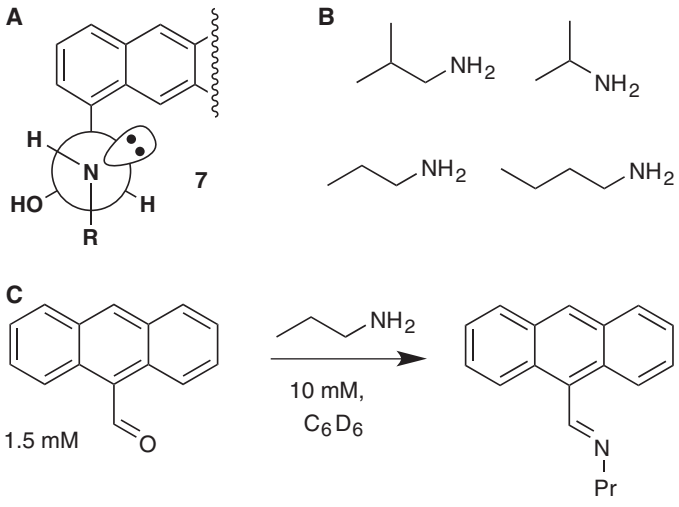

Fig. 4. (**A**) Conformation of the hemiaminal stereocenter inside the complex as viewed down the newly formed N-C bond (one of two possible enantiomers is shown); (**B**) other amines for which hemiaminal formation is observed; (**C**) representation of the cavitand-free control reaction. Pr, propyl group.

tetrahedral intermediates through hydrogen bonding, which also reduces the enthalpic price of the reaction. Accordingly, the cavitand provides a nearly ideal environment for this reaction: The reactants are confined in a limited space and properly oriented, and the desired reactive intermediate is actively stabilized. The stabilization is further enhanced by the binding of the intermediate. In free solution, the dehydration step is self-promoted; in the absence of a better base, a second amine molecule can accelerate the elimination of water. The confinement provided by the cavitand prevents interaction between external base and tetrahedral intermediate, thereby inhibiting progression to the imine.

Are these confining cavities capable of shifting equilibria toward otherwise unstable intermediates (*22*)? Enzyme-catalyzed reactions show enormous rate enhancements through binding to reaction intermediates that structurally resemble transition states. The alteration of equilibria inside enzymes such as triose phosphate isomerase has been proposed (*23*, *24*) but, despite close examination (*25*), has yet to be confirmed. Another proposal relates the magnitude of these effects to the attractive forces between enzyme and substrate, with the greatest effects arising from the formation of covalent bonds (*26*). The evidence presented here supports this view, insofar as the cavitand's functional group arrangement resembles an enzyme active site. Although these cavitands are not catalysts, they show a capacity in stoichiometric quantities to trap reactive intermediates, allowing more direct study of reaction mechanisms.

References and Notes

1. J. Rebek Jr., *Tetrahedron* **35**, 723 (1979).
2. R. I. Masel, *Chemical Kinetics and Catalysis* (Wiley-Interscience, New York, 2001).
3. E. V. Anslyn, D. A. Dougherty, in *Modern Physical Organic Chemistry* (University Science, Sausalito, CA, 2006), ch. 10.
4. D. A. Evans, G. Borg, K. A. Scheidt, *Angew. Chem. Int. Ed.* **41**, 3188 (2002).
5. L. Floriani, E. Marianucci, P. E. Todesco, *J. Chem. Res.* **1984**, 126 (1984).
6. J. A. Chudek, R. Foster, D. Young, *J. Chem. Soc., Perkin Trans. 2* 1285 (1985).
7. D. M. Rudkevich, J. Rebek Jr., *Eur. J. Org. Chem.* **1999**, 1991 (1999).
8. B. W. Purse, P. Ballester, J. Rebek Jr., *J. Am. Chem. Soc.* **125**, 14682 (2003).
9. V. M. Dong, D. Fiedler, B. Carl, R. G. Bergman, K. N. Raymond, *J. Am. Chem. Soc.* **128**, 14464 (2006).
10. M. Ziegler, J. L. Brumaghim, K. N. Raymond, *Angew. Chem. Int. Ed.* **39**, 4119 (2000).
11. M. Yoshizawa, T. Kusukawa, M. Fujita, K. Yamaguchi, *J. Am. Chem. Soc.* **122**, 6311 (2000).
12. T. Iwasawa, E. Mann, J. Rebek Jr., *J. Am. Chem. Soc.* **128**, 9308 (2006).
13. M. Kawano, Y. Kobayashi, T. Ozeki, M. Fujita, *J. Am. Chem. Soc.* **128**, 6558 (2006).
14. D. Fiedler, R. G. Bergman, K. N. Raymond, *Angew. Chem. Int. Ed.* **43**, 6748 (2004).
15. A. Heine *et al.*, *Science* **294**, 369 (2001).
16. E. Lorentzen, B. Siebers, R. Hensel, E. Pohl, *Biochemistry* **44**, 4222 (2005).
17. A. R. Renslo, J. Rebek Jr., *Angew. Chem. Int. Ed.* **39**, 3281 (2000).
18. S. Lin, L. Yang, *Tetrahedron Lett.* **46**, 4315 (2005).
19. T. Gottschalk, B. Jaun, F. Diederich, *Angew. Chem. Int. Ed.* **46**, 260 (2007).
20. R. J. Hooley, J. Rebek Jr., *J. Am. Chem. Soc.* **127**, 11904 (2005).
21. B. W. Purse, A. Gissot, J. Rebek Jr., *J. Am. Chem. Soc.* **127**, 11222 (2005).
22. A. Fersht, *Enzyme Structure and Mechanism* (Freeman, New York, 1984), pp. 47–97.
23. W. J. Albery, J. R. Knowles, *Biochemistry* **15**, 5627 (1976).
24. J. R. Knowles, *Nature* **350**, 121 (1991).
25. S. Rozovsky, A. E. McDermott, *Proc. Natl. Acad. Sci. U.S.A.* **104**, 2080 (2007).
26. X. Zhang, K. N. Houk, *Acc. Chem. Res.* **38**, 379 (2005).
27. We are grateful to the Skaggs Institute and the NIH (grant GM 50174) for financial support. T.I. and R.J.H. are Skaggs Postdoctoral Fellows.

Supporting Online Material

www.sciencemag.org/cgi/content/full/317/5837/493/DC1
Materials and Methods
Figs. S1 to S10
References

2 April 2007; accepted 31 May 2007
10.1126/science.1143272

A Powerful Chiral Counterion Strategy for Asymmetric Transition Metal Catalysis

Gregory L. Hamilton, Eun Joo Kang, Miriam Mba, F. Dean Toste*

Traditionally, transition metal–catalyzed enantioselective transformations rely on chiral ligands tightly bound to the metal to induce asymmetric product distributions. Here we report high enantioselectivities conferred by a chiral counterion in a metal-catalyzed reaction. Two different transformations catalyzed by cationic gold(I) complexes generated products in 90 to 99% enantiomeric excess with the use of chiral binaphthol–derived phosphate anions. Furthermore, we show that the chiral counterion can be combined additively with chiral ligands to enable an asymmetric transformation that cannot be achieved by either method alone. This concept of relaying chiral information via an ion pair should be applicable to a vast number of metal-mediated processes.

The preparation of enantiomerically pure compounds has become a requirement for agrochemical and pharmaceutical synthesis. Such chiral nonracemic compounds are typically accessed from either Nature's "chiral pool," by resolution of a racemate or by means of an enantioselective transformation mediated by a chiral catalyst (*1*). In general, chiral catalysts rely on covalent (dative or nondative) bonds between the reactive site and the chiral moiety. An alternative approach, which takes advantage of the fact that many enantioselective catalysts bear a positive charge, is the induction of asymmetry by interaction of the cationic catalyst with a chiral counteranion associated with the metal in an ion pair. This idea is potentially very powerful because, in principle, the same or a small library of chiral anionic counterions could be used to make a wide range of cationic catalysts enantioselective. The importance of chiral ion pairs is well known in the fields of phase-transfer catalysis (*2*) and organocatalysis (*3*–*6*) and may also be relevant to chiral Brønsted acid catalysis (*7*).

Department of Chemistry, University of California at Berkeley, Berkeley, CA 94720, USA.

*To whom correspondence should be addressed. E-mail: fdtoste@berkeley.edu

Although chiral ions have been successfully applied to the resolution of metal complexes, very few reports have described examining a chiral counterion strategy for metal catalysis (*8*). Support for the concept has been clearly demonstrated; however, the potential has been widely unappreciated because of the low enantioselectivity [0 to 34% ee (enantiomeric excess)] obtained in previous attempts using this method (*9*–*11*). Herein we report a highly enantioselective transition metal–catalyzed reaction mediated by a chiral counterion.

In spite of the recent upsurge of reports documenting reactions catalyzed by homogeneous gold complexes (*12*–*15*), relatively few enantioselective transformations have been discovered (*16*–*22*). Au(I) complexes incorporating chiral phosphines have proven very successful for certain processes but inadequate for others; this deficiency is possibly attributable to the linear coordination geometry of gold, which places the chiral components distant from the substrate. We have previously noted a dramatic effect of the counteranion on the stereoselectivity of cationic Au(I)-catalyzed reactions (*21*). In light of this observation, we envisioned that chiral counterions could provide a particularly advantageous alternative to the traditional chiral ligand approach in the arena of gold chemistry.

Although a number of transition metals catalyze the addition of alcohols across carbon-carbon multiple bonds, to date, only Au(I) complexes have been successful in promoting an asymmetric hydroalkoxylation of allenes (*20*, *23*). Our research efforts, as well as those of others, have found this transformation particularly difficult to achieve with broad substrate scope and high enantioselectivity when using chiral phosphine–ligated catalysts. Only allenol substrates bearing a particular substitution pattern have succumbed to cyclization with high enantioinduction. We therefore saw this reaction as an ideal platform to test the ability of chiral counterions to mediate asymmetric gold reactions.

As expected, for a typical allenol substrate **1**, treatment with a variety of chiral phosphine–substituted gold catalysts in dichloromethane solvent led to poor enantioselectivities (Fig. 1A). In contrast, the catalyst produced in situ from Ph_3PAuCl (in which Ph_3P is triphenylphosphine) and chiral silver phosphate Ag-(*R*)-**6** (*24*, *25*) in dichloromethane solvent furnished a good yield of the hydroalkoxylation product and moderate enantiomeric excess (Fig. 1B). We chose phosphates derived from binaphthol as chiral anions for our investigation because of ease of access and their ready variability (*26*). Moreover, the silver phosphate enables facile generation of the cationic gold(I) catalyst from the phosphinegold (I) chloride driven by precipitation of silver chloride from solution (*27*). Control experiments demonstrated that the reaction is not catalyzed by the phosphoric acid corresponding to protonated **6**, nor is there an appreciable background reaction from either Ph_3PAuCl or the silver phosphate alone. The enantioselectivity of the reaction was improved by utilizing the dinuclear gold complex bearing the bis(diphenylphosphinomethane) ligand (dppm). Examination of other solvents demonstrated that more-polar solvents, such as nitromethane or acetone, gave significantly lower enantiomeric excess values (Fig. 1C). However, the less-polar benzene proved to be the optimal medium, providing the desired product in an exceptional 97% ee. These findings are consistent with an ion-pair model, in which the degree of enantioinduction depends on the proximity of the counteranion to the cationic gold center (*9*).

Knowing the optimized conditions, we explored the scope of the chiral counterion–mediated enantioselective hydroalkoxylation. We found the method could be generally applied to a variety of allenol substrates (Table 1). Different substituents were well tolerated at several positions, including

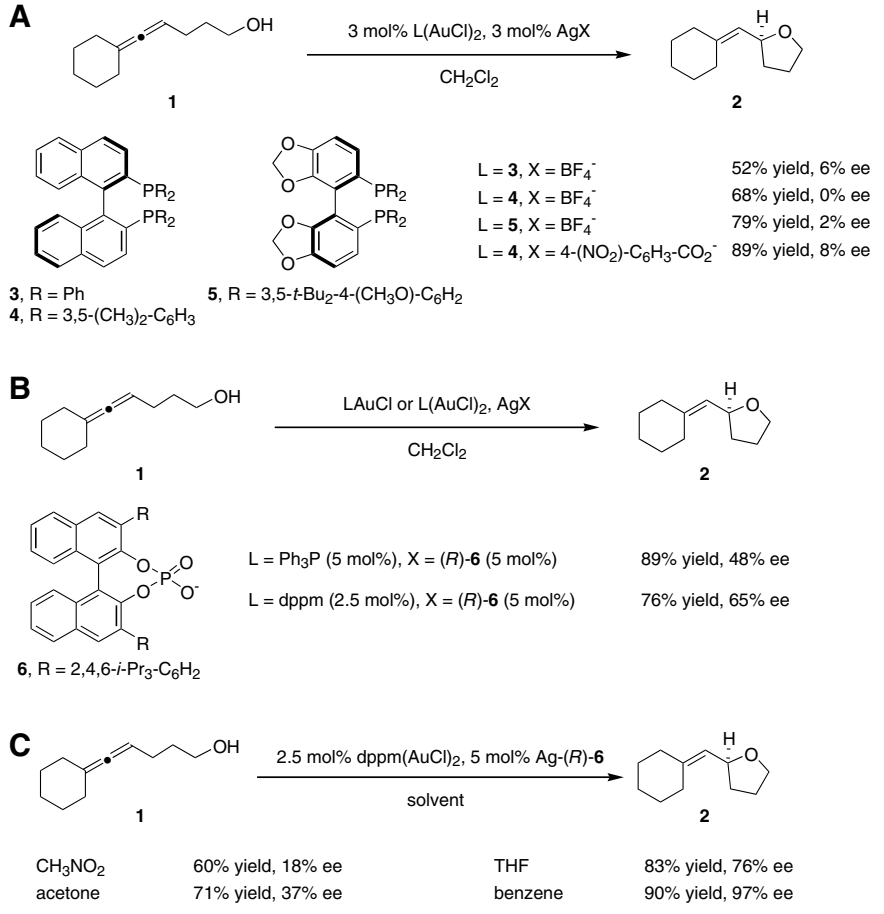

Fig. 1. (**A** and **B**) Comparison of chiral ligands versus chiral counterion for asymmetric hydroalkoxylation. (**C**) Effect of solvent polarity on enantioselectivity.

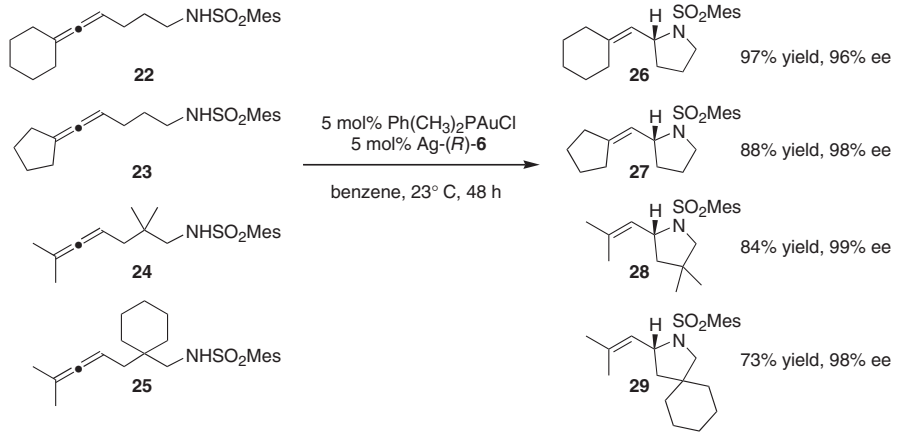

Fig. 2. Counterion-mediated enantioselective hydroamination.

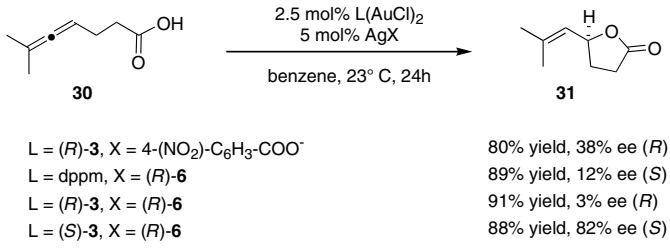

Fig. 3. Hydrocarboxylation using chiral ligand and counterion. The absolute configuration of product enantiomer in excess is noted for each entry.

Table 1. Scope of asymmetric hydroalkoxylation. Entry 8 was performed using (*S*,*S*)-DIPAMP ligand (**7**); enantiomeric excess from using dppm(AuCl)$_2$ is in parentheses. Yields refer to isolated material except for entry 8, which was determined by gas chromatography analysis versus an internal standard.

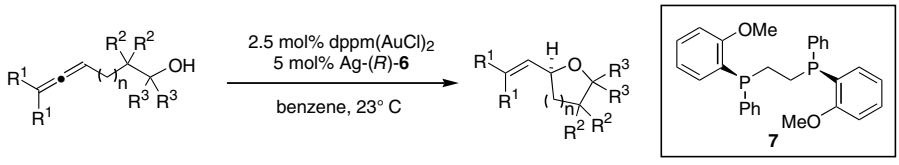

Entry	Substrate	n	R^1	R^2	R^3	Time (h)	Product	% Yield	% ee
1	**1**	1	-$(CH_2)_4$-	H	H	1	**2**	90	97
2	**8**	1	CH_3	H	H	1	**15**	91	95
3	**9**	1	CH_2CH_3	H	H	5	**16**	89	96
4	**10**	1	-$(CH_2)_4$-	H	CH_3	2	**17**	79	99
5	**11**	1	-$(CH_2)_4$-	H	Ph	30	**18**	86	92
6	**12**	1	-$(CH_2)_4$-	CH_3	H	13	**19**	90	90
7	**13**	2	CH_3	H	H	15	**20**	81	90
8	**14**	2	H	H	H	24	**21**	96	92 (80)

the allene terminus (entries 1 to 3) and the α (entries 4 to 5) and β (entry 6) positions of the alcohol. The homologated compound **13** also underwent the reaction to produce tetrahydropyran product **20** with high optical purity.

Even though the achiral ligand system proved successful for a variety of substrates, we were curious to see whether we could combine chiral ligands on gold with the chiral counterion to further improve the enantioselectivity. To study this question, we examined substrate **14**, which lacks any sterically demanding substituents along the backbone or the allene terminus (Table 1, entry 8). This type of unfunctionalized compound is typically very resistant to highly enantioselective transformations, so we were not surprised to find that our standard conditions converted this substrate with slightly reduced enantioselectivity (80% ee). Fortunately, further investigation revealed that combining chiral complex (1*S*,2*S*)-(+)-bis[(2-methoxyphenyl)phenylphosphino]ethane [(*S*,*S*)-DIPAMP](AuCl)$_2$ with Ag-(*S*)-**6** produced the vinyltetrahydropyran product **21** in 92% ee. Pairing the (*S*,*S*)-ligand with the opposite enantiomer of the chiral counterion did not furnish the same improvement in enantioselectivity, indicating that the two combine in a "matched" and "mismatched" fashion. Clearly, the combination of chiral ligands and chiral counterion creates an exceptionally selective system capable of strong enantioinduction for even the most challenging substrates.

Accordingly, we probed the applicability of our chiral counterion strategy to another gold-catalyzed reaction. We considered the intramolecular hydroamination of allenes as a straightforward extension. In the event, we found that a phenyldimethylphosphine-ligated cationic gold complex with the chiral phosphate counterion **6** promoted the desired transformation of allene-sulfonamides with a high level of enantioselectivity (Fig. 2). A number of different substrates performed well under the reaction conditions to give pyrrolidine products in good yield and excellent enantiomeric excess. High enantioselectivity was observed even for compounds **23** and **25**, which gave lower enantiomeric excess values (83% and 70%, respectively) under our previously reported hydroamination conditions in which we used chiral phosphine ligands on gold (*21*). Thus, we have established that the very high enantioinduction from our chiral counterion is not confined to a single reaction, as it offers a useful complementary approach to asymmetric hydroamination of allenes as well.

With these results in hand, we next turned to asymmetric hydrocarboxylation of allenes. Initially, we were disappointed to find that gold complexes incorporating chiral ligands or chiral counterions catalyzed the reaction with poor asymmetric induction (Fig. 3). Nevertheless, we realized this transformation could be an excellent arena in which to test the power of combining chiral ligands and counterions. Despite the extremely low enantioselectivity provided by either component alone, the gold catalyst combining the (*S*)-BINAP [(*S*)-(–)-[2,2′-bis(diphenylphosphino)-1,1′-binaphthyl] ligand [(*S*)-**3**] and (*R*)-**6** counteranion cyclized the allene-carboxylate **30** to lactone **31** in 82% ee. As would be expected, this reaction exhibited a dramatic matched and mismatched pairing effect of the ligand and counterion; the (*R*) enantiomer of the silver phosphate, together with the antipodal (*R*)-BINAP(AuCl)$_2$, produced a nearly racemic product. The highly additive effect of counterion and chiral ligand, as demonstrated here, provides more evidence of the enabling power of the counterion strategy for opening previously inaccessible transformations to asymmetric catalysis.

The chiral counterion approach is especially appealing for Au(I) catalysis, given the aforementioned difficulty of transferring chiral information from a ligand disposed 180° from the substrate. We have shown that modification of the counterion can be used to circumvent this problem by introducing an additional source of chirality near the metal center. Our success relative to previous studies may be partially attributed to the choice of chiral anions that have previously demonstrated potential in asymmetric Brønsted acid catalysis; however, in addition to accessing reactivity not available using Brønsted acid catalysts (*12*), the use of chiral anions in metal catalysis benefits from tuning of the ancillary ligands on the metal in a manner that is not possible for H^+. Moreover, this concept does not preclude processes that require a change in the formal oxidation state of the transition metal catalyst, but rather requires that ion-pairing be maintained in the transition state structure of the enantiodetermining step. Therefore, this approach is by no means limited to cationic gold(I) complexes as catalysts or chiral phosphates as counterions. Considering the multitude of reactions catalyzed by ionic complexes of palladium, rhodium, ruthenium, iridium, and other metals, and given the vast possibilities for chiral anionic and cationic species, we envision tremendous potential in the field of chiral counterion–mediated transition metal–catalyzed reactions. This approach should have especially broad applicability, given that the chiral counterion strategy can be combined with existing chiral ligand platforms in a synergistic fashion.

References and Notes

1. J. Mulzer, in *Comprehensive Asymmetric Catalysis*, E. N. Jacobsen, A. Pfaltz, H. Yamamoto, Eds. (Springer, Berlin, 1999), vol. I, chap. 3.
2. M. J. O'Donnell, in *Catalytic Asymmetric Synthesis*, I. Ojima, Ed. (Wiley-VCH, New York, ed. 2, 2000), chap. 10, pp. 727–755.

3. G. Lelais, D. W. C. MacMillan, *Aldrichim Acta* **39**, 79 (2006).
4. M. S. Taylor, E. N. Jacobsen, *Angew. Chem. Int. Ed.* **45**, 1520 (2006).
5. S. Mayer, B. List, *Angew. Chem. Int. Ed.* **45**, 4193 (2006).
6. N. J. A. Martin, B. List, *J. Am. Chem. Soc.* **128**, 13368 (2006).
7. T. Akiyama, J. Itoh, K. Fuchibe, *Adv. Synth. Catal.* **348**, 999 (2006).
8. J. Lacour, V. Hebbe-Viton, *Chem. Soc. Rev.* **32**, 373 (2003).
9. D. B. Llewellyn, D. Adamson, B. A. Arndtsen, *Org. Lett.* **2**, 4165 (2000).
10. D. B. Llewellyn, B. A. Arndtsen, *Tetrahedron Asymmetry* **16**, 1789 (2005).
11. R. Dorta, L. Shimon, D. Milstein, *J. Organomet. Chem.* **689**, 751 (2004).
12. D. J. Gorin, F. D. Toste, *Nature* **446**, 395 (2007).
13. E. Jiménez-Nunez, A. M. Echavarren, *Chem. Commun.* 333 (2007).
14. A. S. K. Hashmi, G. J. Hutchings, *Angew. Chem. Int. Ed.* **45**, 7896 (2006).
15. L. Zhang, J. Sun, S. A. Kozmin, *Adv. Synth. Catal.* **348**, 2271 (2006).
16. Y. Ito, M. Sawamura, T. Hayashi, *J. Am. Chem. Soc.* **108**, 6405 (1986).
17. M. P. Muñoz, J. Adrio, J. C. Carretero, A. M. Echavarren, *Organometallics* **24**, 1293 (2005).
18. C. González-Arellano, A. Corma, M. Iglesias, F. Sanchez, *Chem. Commun.* 3451 (2005).
19. M. J. Johansson, D. J. Gorin, S. T. Staben, F. D. Toste *J. Am. Chem. Soc.* **127**, 18002 (2005).
20. Z. Zhang, R. A. Widenhoefer, *Angew. Chem. Int. Ed.* **46**, 283 (2007).
21. R. L. LaLonde, B. D. Sherry, E. J. Kang, F. D. Toste *J. Am. Chem. Soc.* **129**, 2452 (2007).
22. C. Liu, R. A. Widenhoefer, *Org. Lett.* **9**, 1935 (2007).
23. For a review on transition metal–catalyzed nucleophilic additions to allenes, see (*28*).
24. When viewed with ^{31}P nuclear magnetic resonance, this gold species in solution is seen to have a chemical shift identical to the catalyst bearing the noncoordinating triflate counterion produced from the combination of Ph_3PAuCl and AgOTf (OTf is trifluoromethane sulfonate), which suggests that a similar cationic species is present in either case.
25. Materials and methods are available as supporting online material on *Science* Online.
26. For a review on chiral phosphoric acids, see (*29*).
27. The catalyst can also be generated by protonation of Ph_3PAuCH_3 with phosphoric acid H-(*R*)-**6** to afford the product in the same yield and enantiomeric excess.
28. R. W. Bates, V. Satcharoen, *Chem. Soc. Rev.* **31**, 12 (2002).
29. S. J. Connon, *Angew. Chem. Int. Ed.* **45**, 3909 (2006).
30. We gratefully acknowledge funding from National Institute of General Medical Services support (R01 GM073932), Merck Research Laboratories, Amgen Inc., Bristol-Myers Squibb, Abbott, Pfizer, DuPont, Novartis, and Boehringer-Ingelheim. We thank Takasago for their generous donation of DTBM-SEGPHOS (**5**). G.L.H. is grateful for an NSF predoctoral fellowship. E.J.K. thanks the Korea Research Foundation Grant (MOEHRD; KRF-2006-214-C00044) and M.M. thanks the University of Padua for postdoctoral fellowships.

Supporting Online Material

www.sciencemag.org/cgi/content/full/317/5837/496/DC1
Materials and Methods
References and Notes

16 May 2007; accepted 13 June 2007
10.1126/science.1145229

A Cambrian Peak in Morphological Variation Within Trilobite Species

Mark Webster

Morphological variation within species is a raw material subject to natural selection. However, temporal change in morphological diversity has usually been studied in terms of variation among rather than within species. The distribution of polymorphic traits in cladistic character-taxon matrices reveals that the frequency and extent of morphological variation in 982 trilobite species are greatest early in the evolution of the group: Stratigraphically old and/or phylogenetically basal taxa are significantly more variable than younger and/or more derived taxa. Through its influence on evolutionary tempo, high intraspecific variation may have played a major role in the pronounced Cambrian diversification of trilobites.

Many higher taxa show a markedly asymmetric diversification history, with rapid initial increase in morphological diversity among taxa (disparity) and subsequent decline in or cessation of evolutionary inventiveness (*1*–*4*). Rates of taxonomic diversity increase are also often higher during the early portion of clade evolutionary history (*5*, *6*). Because the potential rate and magnitude of evolutionary change (evolvability) for a species must be to some extent a function of the degree of morphological variation exhibited by that species (*7*, *8*), change in the frequency or nature of intraspecific variation within a clade could profoundly influence its evolutionary dynamics. To the extent that observed phenotypic variation reflects heritable variability (*7*) and therefore evolvability, a clade exhibiting a bottom-heavy diversification history would be predicted to show a temporally declining degree of intraspecific variation among its constituent members, as has been claimed for some animal clades ["Rosa's Rule" (*9*, *10*)].

Here I investigate long-term trends in morphological variation in species using the 270-million-year history (Early Cambrian through Late Permian) of trilobites. Trilobites have a character-rich morphology, abundant fossil record, and high diversity. The diversification history of trilobites was bottom-heavy (fig. S1A): Origination and extinction rates of trilobite genera were generally higher in the Cambrian than later (fig. S1, B and C), although there was rapid diversification within some post-Cambrian clades (*11*). Maximal disparity was achieved during the Early Cambrian [based on among-species variation in thoracic segment number (*12*)] or the Ordovician [based on among-species variation in cranidial outline (*6*, *13*) and qualitative assessment of gross anatomy (*14*)]. Although it has been suggested that the net decline in evolutionary rate corresponded to a general decrease in morphological variability within trilobite species through time (*15*, *16*), the few pertinent studies to date do not provide strong empirical support for unusual variation within Cambrian trilobite species in any aspect of morphology other than number of thoracic segments at maturity [(*12*); see supporting online material (SOM)], and even that trait is variable within only very few species.

I explored temporal patterns in intraspecific variation as represented by character states coded as polymorphic within trilobite species in cladistic analyses. Species coded as polymorphic for a given character are assumed to have exhibited marked variation that spanned two or more states defined by the original authors. Aspects of organismal shape, counts of meristic features (including presence or absence of particular features), and locations and discrete types of particular anatomical structures can all form the basis for characters coded in cladistic analyses, thus maximizing morphological coverage (SOM).

I examined 68 trilobite character-taxon matrices for intraspecific polymorphisms (table S1), but application of stringent criteria to reduce the potential for among-study bias (*17*) resulted in exclusion of some entire matrices, and of particular characters and/or taxa from others (table S1). The final data set consisted of character-taxon matrices from 49 independent studies (tables S1 and S2). Character-state information for a total of 982 species was included (table S2), representing ~5% of all valid trilobite species (*18*). All eight orders of trilobites, plus the problematic burlingiids, were represented. I treated agnostids as trilobites (*19*–*21*), but my general conclusions are not dependent upon their inclusion. All orders were represented by more than 100 species in the analysis, with the exception of the Redlichiida (79 species), the Corynexochida (50 species), and the Asaphida (26 species). With the exception of the Permian, geologic periods were subdivided into two or three temporal bins (typically corresponding to epochs); the stratigraphic age at this finer level of resolution was known for 957

Department of the Geophysical Sciences, University of Chicago, 5734 South Ellis Avenue, Chicago, IL 60637, USA. E-mail: mwebster@geosci.uchicago.edu